Numerical Simulation Of The Flow Noise Of A Finite Circular Cylinder

Schneehagen, Erik W.[1]
Institute of Fluid Mechanics and Engineering Acoustics
TU Berlin, Einsteinufer 25, 10587 Berlin, Germany

Zhou, Beckett Y.[2]
Chair for Scientific Computing
TU Kaiserslautern, Bldg/Geb 34, Paul-Ehrlich-Strasse, 67663 Kaiserslautern, Germany

Sarradj, Ennes [3]
Institute of Fluid Mechanics and Engineering Acoustics
TU Berlin, Einsteinufer 25, 10587 Berlin, Germany

ABSTRACT

For many engineering applications flow generated noise is a relevant component of the total sound. The prediction of the flow noise is often not easy because of the high complexity of the turbulent flow field. Even with increasing computational power and for simple geometries, the direct numerical simulation is often too expensive because of the big difference in acoustic and fluid length scales. A possible solution is the separate calculation of the flow field and the acoustics. A known hybrid approach is the combination of a large eddy simulation (LES) with the acoustic analogy of Ffowcs-Williams-Hawkings (FW-H). The realization of this method with two different open source CFD codes is presented. The simulation of the flow field is performed with SU2 and OpenFOAM respectively and used for the calculation of flow noise of a finite wall-mounted circular cylinder configuration. Simulation results are compared to measurement data from an aeroacoustic wind tunnel and other available data from simulations and measurements.

Keywords: Flow noise, Numerical acoustics
I-INCE Classification of Subject Number: 76

---

[1] erik.w.schneehagen@tu-berlin.de

[2] yuxiang.zhou@scicomp.uni-kl.de

[3] ennes.sarradj@tu-berlin.de

1. INTRODUCTION

In this work an aeroacoustic prediction of the flow-induced noise of a wall-mounted circular cylinder is performed using a hybrid approach where the flow field and the acoustics are calculated separately. This flow configuration is well suited for validation purposes because it is has complex three dimensional flow with a quite simple geometry. The Reynolds number is 20,000 based on the cylinder diameter of 8 mm and the free stream velocity of 36.7 m/s. For this Reynolds number the flow is in the subcritical regime. The aspect ratio (AR) of the cylinder is 6. The results from the flow simulation are compared to experimental data from Park and Lee (2002) [1] and data from a LES performed by Afgan et al. (2007) [2] who both investigate the same aspect ratio cylinder under the described flow conditions. Because there is no acoustical data available for this case an acoustic measurement is performed to validate the simulation. The long term goal of this research is to investigate the influence of the tip geometry on the flow noise. The chosen dimensions for the computational domain for the flow setup can be seen in Figure 1 with the coordinate system in red. The blockage for this configuration is 2.2 %.
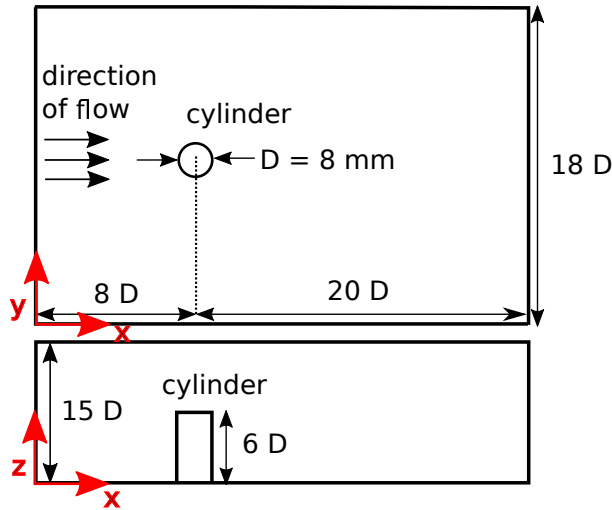

Figure 1: setup of the computational domain for the flow configuration, top and side view, coordinate system in red

2. COMPUTATION

For this hybrid approach the flow field solution is calculated first and then the dynamic pressure on the rigid surface is used as acoustic source terms. For obtaining the instationary flow field a large eddy simulation (LES) is performed. By low-pass filtering the Navier-Stokes equations only the large scales of the flow field get resolved. The smaller scales need to be modeled. This can either be done *implicitly* where below the grid resolution of the mesh numerical dissipation mimics the viscosity of the fluid or *explicitly* by introducing a subgrid-scale model which represents the physics of the small scale motions. In SU2 an implicit LES is available and for OpenFOAM an explicit LES is used. The details of the numerical set up are described in the following sections.

2.2.1. Flow simulation SU2

The SU2 software suite [3] is an open-source collection of software tools written in C++ and Python designed for multi-physics simulation and design. It is built specifically for the analysis of partial differential equations (PDEs) and PDE-constrained optimization problems on unstructured meshes with state-of-the-art methods and algorithms. The finite volume method (FVM) is applied on arbitrary unstructured meshes using a standard edge-based data structure on a dual grid with control volumes constructed using a median-dual, vertex-based scheme. Regarding time integration, SU2 is capable to solve implicitly steady and unsteady problems, using a dual-time stepping strategy, leading to second-order accuracy in space and time. The numerical flux scheme used is the Simple Low-dissipation AUSM (SLAU2) scheme [4]. Recently SU2 solver has been used to perform aeroacoustic prediction of the tandem cylinder configuration and validated against experiment [5]. The SLAU2 scheme is used for its low dissipation properties which allows Kelvin-Helmholtz instability in the shear layer to develop quickly into plausible turbulence

The computation is initialised with a homogeneous flow field with a velocity of 36.7 m/s. The cylinder surface has a no-slip boundary condition. For the wall on which the cylinder is mounted a slip boundary condition is chosen. For an aspect ratio 6 the incoming boundary layer should not have a huge influence on the total flow field. This assumption saves a lot of computational cost because no boundary layer on the wall has to be resolved. For all other sides of the computational domain the *far field* boundary condition is applied.
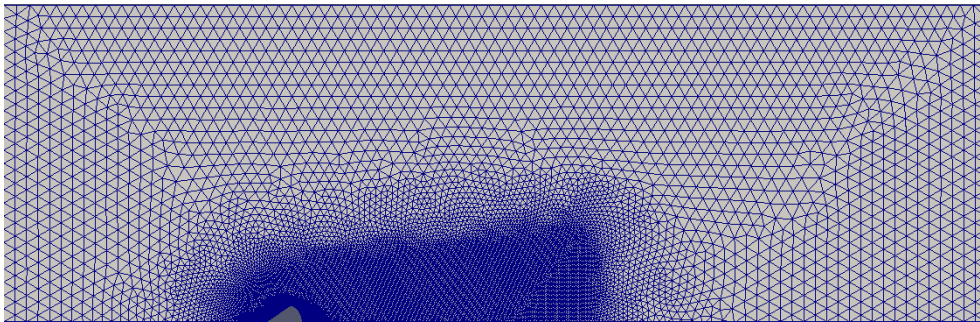

Figure 2: Bottom view of computational mesh used for SU2, cut along the symmetry line, refinement in the wake of the cylinder, flow direction left to right

For the computation a hybrid mesh is created with the open source meshing software SALOME. The mesh consists of 4.2 million points. Around the cylinder a boundary layer of structured prisms is applied so that the dimensionless wall distance $y+$ is smaller than 1 for the described flow conditions. The rest of the mesh is unstructured and consists of tetrahedrons. The refinement zone downstream of the cylinder can be seen in Figure 2.

2.2.2. Flow simulation OpenFOAM

OpenFOAM is a open-source C++ toolbox which also uses the FVM. For this computation a LES with the Smagorinsky-model [6] is used. In OpenFOAM v1712 the turbulent viscosity is implemented as

$$\nu_t = C_k \Delta k^{0,5}. \tag{1}$$

It is dependent on a model constant C_k, the filter width Δ and the turbulent kinetic energy k. For C_k the default value of 0.094 from the OpenFOAM documentation is used. The filter width Δ depends on the grid resolution and is the geometrical mean value of the three spatial coordinates of a control volume. The simulation uses the PISO-algorithm for incompressible flows. An inlet boundary condition with a homogeneous velocity of 36.7 m/s is used. For the outlet the pressure is set to 0. The cylinder surface has again a no-slip boundary condition. On the bottom a slip boundary condition is applied with the same justification as argued above. The other three sides of the domain also have slip boundary condition. The turbulent viscosity is set to *zeroGradient* at all boundaries.

For this simulation a different mesh has to be used because the available spatial filters show unphysical behaviour for the tetrahedral mesh which is used for the SU2 simulation. Therefore a structured hexahedral mesh is created with the OpenFOAM routine *snappyHexMesh*. To make the meshes and results comparable the same amount of grid points (4.7 mio) is used. Also a boundary layer is applied on the cylinder surface. The height of the cells closest to the cylinder is chosen so that the dimensionless wall distance *y+* is almost everywhere below 1.5. Figure 3 shows how the mesh is gradually refined in the wake of the cylinder.
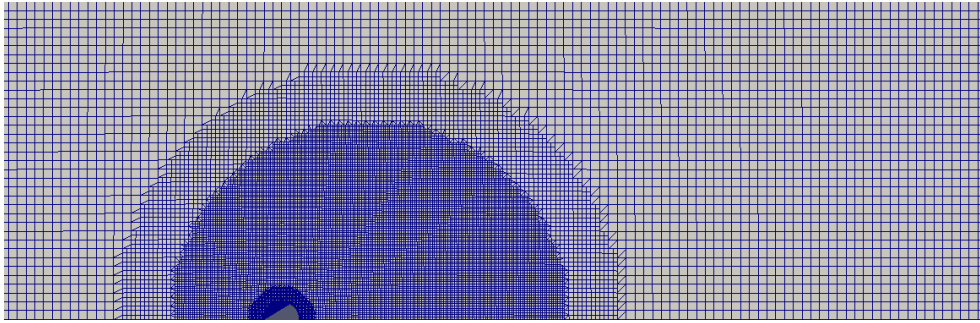

Figure 3: Bottom view of computational mesh used for OpenFOAM, cut along the symmetry line, circular refinement zone around the cylinder, flow direction left to right

2.2.3. Acoustics

For the calculation of radiated sound the FW-H equations [7] are used with some simplifications. Because the cylinder and the wall are not moving the monopole like term of the FW-H equations vanishes. Additionally the contribution of the quadrapole term which corresponds to the turbulent shear stresses in the surrounding volume can be neglected for low Mach number flows. In this setup with a Mach number of 0.105 this is a reasonable assumption. For the acoustical computation it is therefore sufficient to only consider the sound radiation from the forces acting on the solid surface because of the time varying pressure fluctuations p_g from the flow. The acoustical pressure fluctuations p_L can be calculated as

$$p_L(\boldsymbol{x},t) = \frac{1}{4\pi c} \frac{\partial}{\partial t} \int_{f(\boldsymbol{x})=0} \frac{p_g(\tau_0)\boldsymbol{n}\boldsymbol{e_r}}{r} \mathrm{d}\boldsymbol{S}, \qquad (2)$$

where $\boldsymbol{n}$ is the normal vector of the surface element $\boldsymbol{S}$. The unity vector $\boldsymbol{e_r}$ points to the observer location $\boldsymbol{x}$ which has the distance r. The control surface $f(x)$ is the impenetrable surface of the cylinder. The retarded time τ_0 takes in account the different propagation times from source to observer.

In both simulations the pressure fluctuations in the mesh points on the cylinder surface are stored with a sampling frequency of 10 kHz. For this cloud of points the Delaunay-algorithm is used to calculate triangles which make up the cylinder surface. So the integration from Equation 2 becomes a summation of the products of triangle area and interpolated pressure fluctuations in the centroids for every time step. The time derivative is implemented as a simple difference quotient. For the retarded time the minimum distance is calculated and the time signal for every centroid is shifted according to minimum time resolution.

3. ACOUSTICAL MEASUREMENT

The acoustical measurements are performed at the aeroacoustic wind tunnel at B-TU Cottbus-Senftenberg. In Figure 4 the setup at the free stream test section is shown. The green rectangle is the frame of the nozzle exit (w 0.23 m x h 0.28 m) where an acrylic glass plate is attached to. The cylinder is mounted to the plate with a distance of 0.1 m to the nozzle exit. The surrounding walls are covered with porous material and are acoustically fully absorbent above 250 Hz. The acoustic pressure fluctuations are recorded with three 1/4" free field condenser microphones located left, right and above the cylinder at the same downstream position as the cylinder. The signals are recorded for 60 s with a sampling frequency of 51.2 kHz. The measurement is done once with the cylinder mounted to the wall and once without it. This is done in order to distinguish between the noise belonging to the operation of the test facility and the sound produced by the cylinder. The blockage for this setup is 0.5 %.
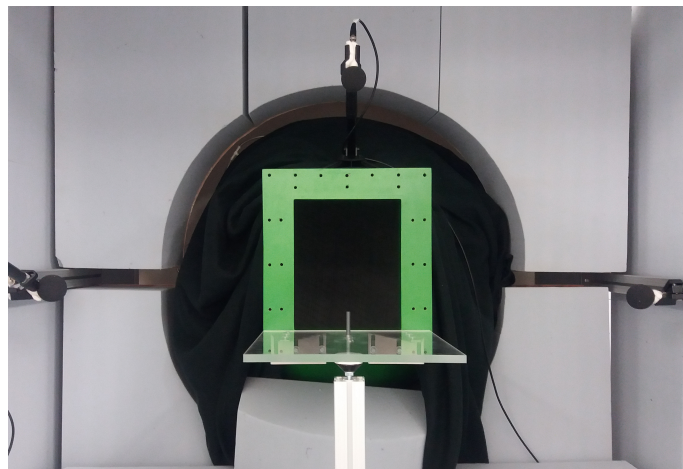

Figure 4: Setup aeroacoustic wind tunnel, cylinder in the middle on mounting wall attached to the nozzle (green), microphones to the left, top and right

4. DISCUSSION OF RESULTS

In order to decide if the LES is past the transient phase the running average of the lift and drag coefficient are monitored. Once the behaviour reaches a quasi periodic stationary state the data collection begins. All the values shown in the next sections are for a simulation length of 25 flow through times (0.16 s) from this point on. The flow through time is the time that a particle needs to cross the computational domain streamwise with the mean flow velocity. The relevant flow information is stored every 0.1 milliseconds.

The results of the flow simulation are compared to the measurements from Park and Lee (2002) [1] and the simulations of Afgan et al. (2007) [2]. The acoustical results are compared to the measurements from the aeroacoustic wind tunnel.

4.4.1. Flow results

In the LES of Afgan et. al (2007) and of course in the measurement of Park and Lee (2002) a boundary layer is present on the mounting wall of the cylinder. Because friction on the wall is not included in the SU2 and OpenFOAM simulation the comparison of the flow results is done in a minimum distance of half the cylinder height from the wall. Because the boundary layer thickness in the experiment is only $\delta \sim 6\%$ D the other flow features should be more dominant and not too much affected by the wall at these locations.

Figure 5 shows the circumferential pressure coefficient on the cylinder surface for different angles at different heights. The simulation data is compared to measurement from Park and Lee (2002). In their set up 19 pressure tabs are vertically placed in the cylinder surface and the cylinder is rotated in 10° increments. The reference pressure for the simulations is normalized so that in the stagnation point at 0 degrees the simulations have the same value for C_P as the measurement.

In the left part of the figure the pressure distribution is shown at half the cylinder height. The SU2 simulation (red) is in quite close agreement with the measurement (black). The pressure drop is a bit smaller but located at the same point and has the same shape. For the OpenFOAM simulation (blue) the lowest pressure is at a higher angle and the recovery to the pressure plateau is reached more slowly. The value is also higher as in the SU2 simulation. At the vertical cylinder location z/L = 0.75 the results from SU2 are
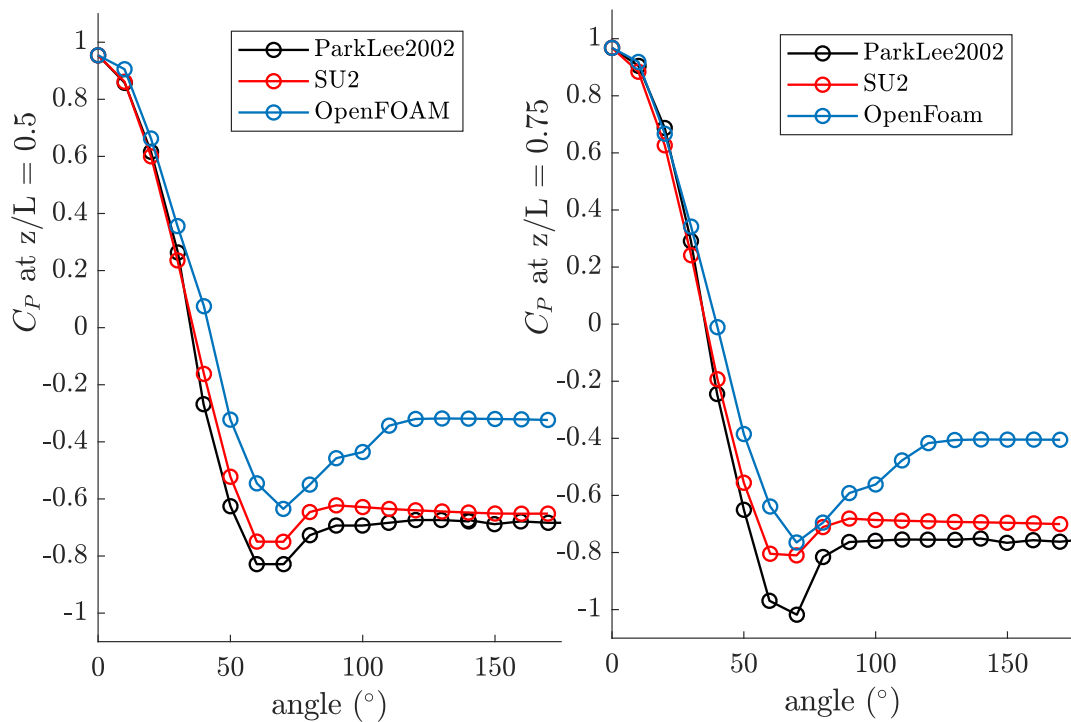

Figure 5: Circumferential pressure coefficient at different heights on the cylinder surface compared to measurement data from Park and Lee (2002)

again closer to the measurement. Although the pressure drop in the measurement is more drastic, the shape of the pressure recovery looks qualitatively similar. For this location OpenFOAM correctly predicts the angle of of the point with the lowest pressure but the recovery is once more slower and the pressure plateau has a lower level. A possible reason why the results tend to get worse when moving closer to the top is that the shear layer behind the tip is not resolved well enough. This could affect the prediction of the downwash from the cylinder tip and hence the pressure on the surface.

In Figure 6 the average streamwise velocity normalized by the mean free stream velocity in five diameters distance to the cylinder is shown. The left graphs are for a height of $z/L = 0.5$ and the right for $z/L = 0.75$ where $z/L = 0$ would be the wall. In the left part of Figure 6 it can be seen that the minimum of the velocity profile of the SU2 simulation (red) is at 0.55 and slightly higher than the results from the LES (black) of Afgan et al. (2007) which show the minimum at a value of 0.5. The OpenFOAM results (blue) show a similar velocity distribution along the y-axis as the other two but the minimum is a bit higher at 0.66. This means that the width of the wake behind the cylinder is predicted correctly. The strength of the recirculation on the other hand is quite low for the OpenFOAM simulation. SU2 shows good agreement for this case. In the
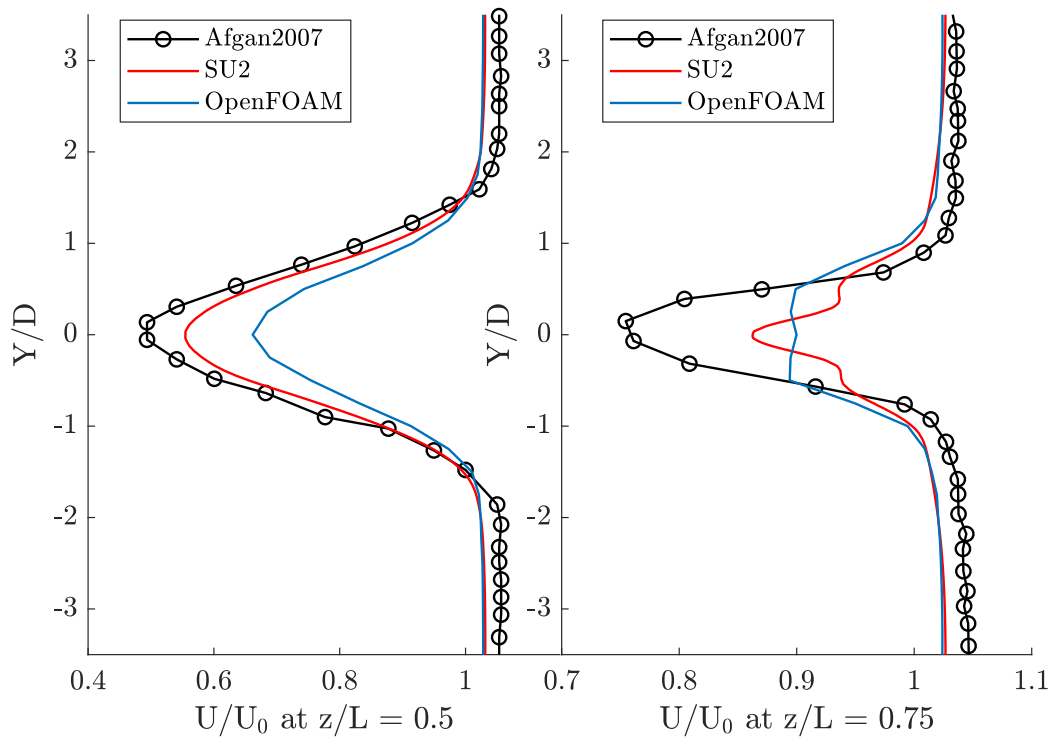

Figure 6: *Comparison of the normalized streamwise mean velocity at different heights, notice different scales on the axis for U/U_0*

right part of Figure 6 the same quantity is shown at a height of $z/L = 0.75$. The velocity profile of the OpenFOAM simulation is more blunt and the minimum is around 0.9. The wake is wider as in the simulation from Afgan et al. (2007). In this simulation the minimum of the velocity profile is 0.76. The SU2 simulation also shows a different shape of the wake and the minimum is not as low as in the measurement. It can be again seen that the results closer to the top have a relatively larger difference than the results at the

midspan. It seems that further mesh refinement at the tip is required to correctly capture the downwash and vortices at the top.

In Figure 7 the streamwise turbulence intensity in five diameters distance to cylinder at a height of $z/L = 0.5$ is shown. The midspan of the cylinders lies at $Y/D = 0$. The turbulence intensity of the hot wire measurements of Park and Lee (2002) has a maximum of 28 % at the centerline while the LES results from Afgan et al. (2007) show to maximums of 26 % symmetrical to the centerline. The latter behaviour can also be found in the results of the SU2 (red) and OpenFOAM (blue) simulations. Both show similar shapes but also underpredict the streamwise turbulence intensity. The maximum of SU2 lies around 24% and the OpenFOAM simulation is the lowest with 20%.
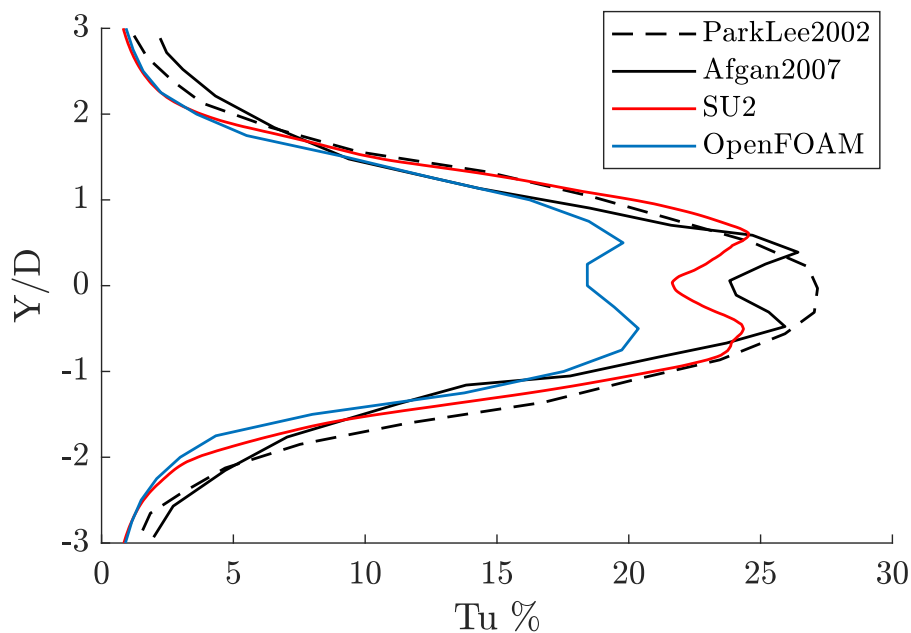

Figure 7: Streamwise turbulence intensity at X/D = 5 for at half the cylinder height (z/L = 0.5) compared to hot wire measurements of Park and Lee (2002) and LES results of Afgan et. al (2007)

4.4.2. Acoustic results

In Figure 8 the power density spectra of the measurement with the cylinder in the flow (green) and without the cylinder in the flow (red) are shown. The difference of the spectrum of the squared sound pressure values of both runs is shown in black. It can be subtracted under the assumption that the operating noise of the test facility is stationary. The spectrum is only evaluated for frequencies where the level difference of these two measurements is above 3 dB and starts therefore at 600 Hz and ends around 2,600 Hz. In the frequency range of the peak the difference was around 6 dB. This means that the absolute level of the peak can be well distinguished from any other noise sources. For better comparison to the simulation results the level in the spectra are divided by the frequency resolution. The spectra are averaged with Welch's method for a window length of 4096 samples resulting in an average over 750 windows using a Hanning window with 0.0 overlap.
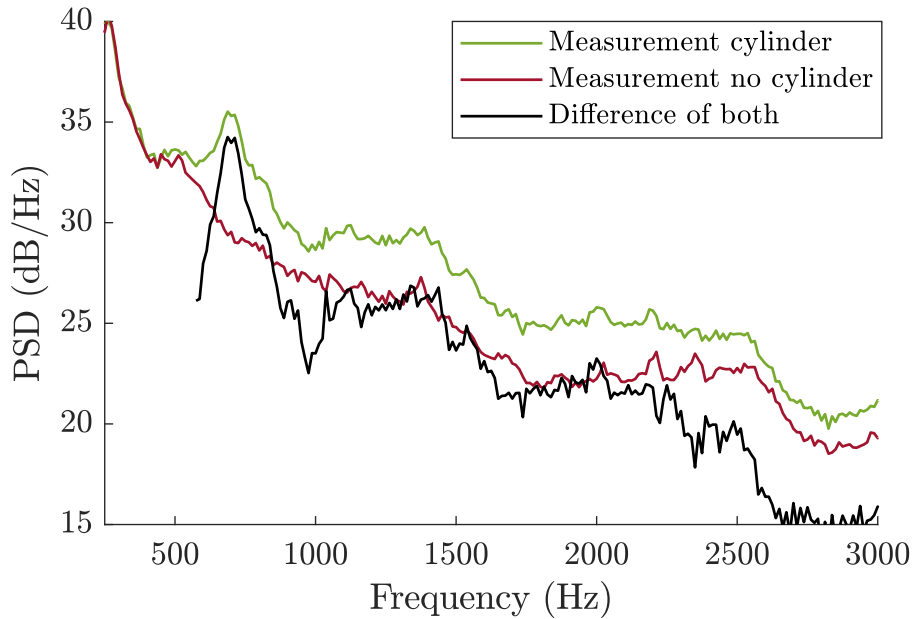
Figure 8: Power density spectra from the measurement with and without the cylinder in the flow and the difference for both for Re = 20,000

In Figure 9 the computed emitted sound of the cylinder surface is compared to the data from the wind tunnel measurement. The observer location for the computation has relatively to the cylinder the same distance as the microphone in the measurement. The frequency resolution from the simulation data is coarser because the computation of the flow field solution is expensive. The length of the computed pressure time signal is only 0.16 s. The computed spectra are averaged over 12 time windows with a sample length of 128. For all three spectra a Hanning window with 0.0 overlap is again used. It can be clearly seen that both simulations underpredict the sound pressure level. The OpenFOAM simulation (blue) shows the peak at the shedding frequency of 700 Hz. The level is around 3 dB lower at the peak and around 5 dB to 8 dB lower in the rest of the spectrum. Apart from the offset the OpenFOAM result shows a similar spectrum.

The SU2 spectrum (red) shows a less prominent peak which is also broadened. The level difference at the peak is around 15 dB and in the rest of the spectrum it lies roughly between 12 dB and 20 dB. The overall sound pressure level (OASPL) from 600 Hz to 2600 Hz is also shown in Table 1. The OpenFOAM results show a 4 dB lower level and the SU2 results are 14 dB lower. This large difference is surprising because the SU2 simulation show better results in the comparison of the flow data.

Table 1: Comparison of overall sound pressure level (OASPL) from 600 Hz to 2600 Hz and the RMS value of the lift coefficient C_L

	Measurement	SU2	OpenFOAM
OASPL (dB)	59.1	45.5	55.4
C_{Lrms}	-	0.012	0.0239

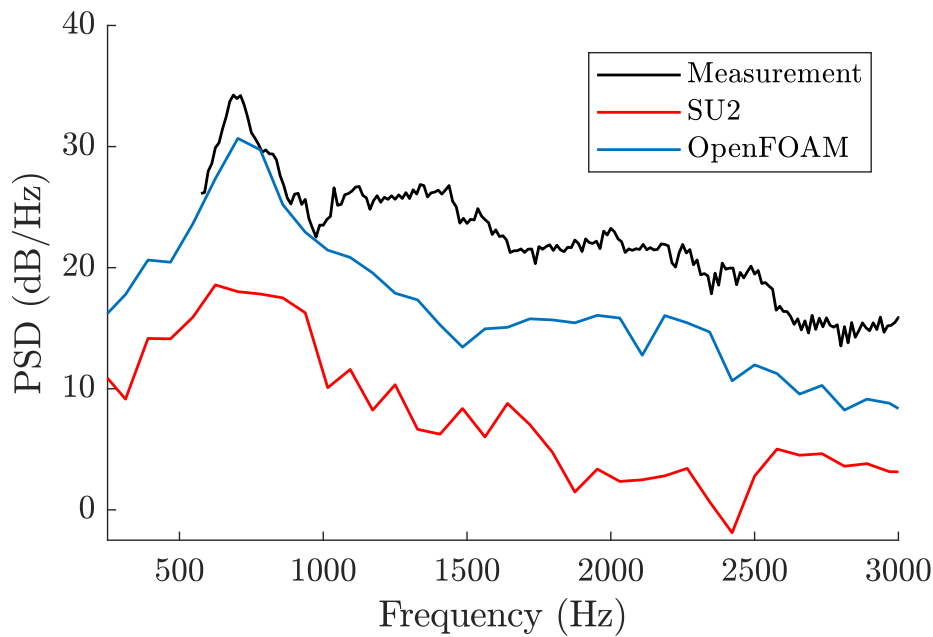Before discussing possible reasons for this discrepancy it should be addressed which

Figure 9: Comparison of power density spectra at the same observer location for measurement and simulation for Re = 20,000

limits the acoustical simulation has in general. First of all the integral formulation from Equation 2 does not include any reflecting surfaces along the propagation path. In the measurement thy cylinder is attached to an acrylic plate with a width of 0.23 m and a length of 0.3 m. These reflections are not included in the computation. Even though the Helmholtz number is only around 0.5 at the shedding frequency for the wall dimensions it might be a factor for higher frequencies. Potentially it could make difference up to 6 dB in sound pressure level. For this case it will be a lot smaller though. Furthermore as argued above the wall has a slip boundary condition. For this reason the sound radiated by the wall because of the dynamic surface pressure fluctuations is not included. Others simulations carried out by the author showed for similar setups that the contribution from the wall is small in comparison to the shedding tone radiated by the cylinder. Still the noise level could be elevated by a few dB when the wall is included.

These errors apply to both simulations though and only explain differences regarding the measurement. The obvious sound pressure level difference of 10 dB between the simulations needs to have other reasons. In Table 1 the RMS value of the lift coefficient is listed. The projected area of the cylinder is used as the reference area. The value for the SU2 simulation is about half the value from the OpenFOAM simulation. This means that the force acting on the cylinder surface because of the vortex shedding is only half as strong. For low frequencies and harmonic signals the acoustic pressure amplitude at the observer location is directly proportional to force acting on the cylinder surface. For a 50 % lower force this results in a sound pressure level that is 6 dB lower. The reason why the force is lower in the SU2 simulation is not clear yet and needs to be investigated more deeply. It is surprising that the velocity related quantities are better captured by the SU2 simulation but the pressure related force is a lot lower resulting in a lower sound pressure level.

5. CONCLUSION

In summary the flow results are in satisfactory agreement with the compared data. The SU2 simulation shows better agreement with the compared quantities especially for the pressure coefficient. For both simulations the results tend to get worse closer to the tip. This problem will addressed in future simulations by refining the computational grid in the region of the tip to capture the downwash effects occurring there. Also a boundary layer on the mounting wall of the cylinder will be included to add an incoming boundary layer for the cylinder flow. The hybrid approach of calculating the acoustic separately from flow works quite well for the OpenFOAM simulation. The overall sound pressure level is underpredicted by 4 dB in comparison to the wind tunnel measurement. This encourages to believe that the results can be further improved when the reflection from the mounting surface and the sound radiation from the wall are also included. The latter will be added in future simulations when the boundary layer is introduced at the wall. On the other hand the prediction of the sound pressure level from the SU2 results shows a big discrepancy of 14 dB. This can be partly explained by the underpredicted force acting on the cylinder surface. The reason why the force is too low is not found yet and needs further investigation.

6. ACKNOWLEDGEMENTS

7. REFERENCES

[1] S.J. Park, C.W. Lee. Flow structure around a finite circular cylinder embedded in various atmospheric boundary layers. *Fluid Dynamics Research*, 30(3):197–215, 2002.

[2] I. Afgan et al. Large eddy simulation of turbulent flow for wall mounted cantilever cylinders of aspect ratio 6 and 10. *International Journal of Heat and Fluid Flow*, 28:561–574, 2007.

[3] Economon, T. D., Palacios, F., Copeland, S. R., Lukaczyk, T. W., and Alonso, J. J. SU2: An open-source suite for multiphysics simulation and design. *AIAA Journal*, 54(3):pp. 828–846, 2016.

[4] Kitamura, K., and Hashimoto, A. Reduced dissipation AUSM-family fluxes: HR-SLAU2 and HR-AUSM+-up for high resolution unsteady flow simulations. *Computers & Fluids*, Vol. 54:pp. 828–846, 2016.

[5] E.S. Molina, B.Y. Zhou, J.J. Alonso, M. Righi, R. G. Silva. Flow and noise predictions around tandem cylinders using DDES approach with SU2. *AIAA-2019- 0326, AIAA SciTech Forum, San Diego, California*, January 2019.

[6] J Smagorinsky. General circulation experiments with the primitive equations: I. the basic experiment. *Monthly weather review*, 91(3):99–164, 1963.

[7] J. Ffowcs Williams and D. Hawkings. Sound generated by turbulence and surfaces in arbritary motion. *Philosophical Transactions of the Royal Society of London*, Vol. 264(No. 1151):321–341, 1969.